 CMES, vol.78, no.2, pp.95-108, 2011

Higher-Order Green's Function Derivatives and BEM Evaluation of Stresses at Interior Points in a 3D Generally Anisotropic Solid

Y.C. Shiah[1] **and C. L. Tan**[2]

Abstract: By differentiating the Green function of Ting and Lee (1997) for 3D general anisotropic elastotatics in a spherical coordinate system as an intermediate step, and then using the chain rule, derivatives of up to the second order of this fundamental solution are obtained in exact, explicit, algebraic forms. No tensors of order higher than two are present in these derivatives, thereby allowing these quantities to be numerically evaluated quite expeditiously. These derivatives are required for the computation of the internal point displacements and stresses via Somigliana's identity in BEM analysis. Some examples are presented to demonstrate their successful implementation to this end, in which the numerical results are compared with corresponding values obtained using the finite element method (FEM). An assessment of the relative efficiency of the BEM analysis when using the present exact form of the derivatives versus another previous exact form is also presented.

Keywords: Boundary element method, Green's functions, boundary integral equations, Somigliana's identity, anisotropic elasticity, Stroh's eigenvalues.

1 Introduction

The displacements and stresses at interior points of a solid are sometimes required in elastic stress analysis. Examples include more detailed examination of the variations of these quantities near stress concentrations and in the determination of the fracture parameters, J- or M-integrals, in fracture mechanics analysis. As the boundary element method (BEM) is a boundary solution numerical technique, these interior point solutions are obtained as a secondary procedure after the boundary integral equation (BIE) has been solved. It entails evaluating Somigliana's identity for displacements; the corresponding identity for the stresses can be obtained by

[1] Dept. of Aerospace and Systems Engineering, Feng Chia University, Taichung, Taiwan, R.O.C.
[2] Dept. of Mechanical & Aerospace Engineering, Carleton University, Ottawa, Canada K1S 5B6

differentiating this identity for the strains and invoking Hooke's law. Although this is well established in BEM for isotropy and 2D general anisotropy, the authors are not aware of any similar implementation for 3D general anisotropy in the literature. This is because of the mathematical complexity of the fundamental solution for the 3D problem and its higher order derivatives required.

In the previous BETEQ2010 meeting, the present authors reported an improved BEM formulation for 3D generally anisotropic elastic solid based on fundamental solutions which are real-variable and fully algebraic in form, Shiah *et al* (2010a). The availability of the fundamental solution and its derivatives in closed, algebraic form makes their implementation into an existing BEM code a relatively straightforward task, without the need to develop special algorithms for their evaluation. The Green's function for displacements employed was that by Ting and Lee (1997); the corresponding fundamental solution for tractions was obtained by the present authors using a revised approach that was recently presented by Lee (2009) for analytically obtaining the first derivatives of the Green's function. The approach for getting these first derivatives obviate the introduction of high order tensor terms present in the traction fundamental solution that was used in a similar BEM formulation developed previously, Tan *et al* (2009). It was found in the course of the work reported in Tan *et al* (2009) that the evaluation of these high order tensors expends a disproportionate amount of the numerical effort. Their absence in the revised formulation significantly improves the computational efficiency, as demonstrated in Shiah *et al* (2010a). The revised approach of Lee (2009) also enables higher order derivatives of the Green's function to be obtained without introducing the very high order tensors, although no explicit expression of any of them is analytically derived and presented. It should be noted here, however, that different algorithms for computing higher order derivatives of the Green's function for general anisotropy have also been presented recently by other authors in their BEM work, although the focus of these works is different from that of the present study. Benedetti *et al* (2009) in their development of fast dual BEM for 3D anisotropic, elastic crack problems employed the non-explicit form of the Green's function by Lifshitz and Rosenzweig (1947), and adopted the interpolation algorithm of Wilson and Cruse (1978) to obtain the approximate numerical values of this fundamental solution and the derivatives. Buroni and Saez (2010), on the other hand, derived a general algebraic expression for the second order derivatives of the Green's function by Ting and Lee (1947) using the approach presented in Shiah *et al* (2009). As expected, it contains terms that are 10^{th} order tensors and the fully explicit forms of which were not presented. These high order tensors are the quantities that the present authors have successfully strived to avoid in developing the algorithm for evaluating internal point stresses in 3D anisotropic elastic bodies using Somigliana's identity.

Using the revised approach of Lee (2009), the present authors have recently derived the explicit algebraic forms of the second derivatives of the Green's functions in terms of Stroh's eigenvalues without the very high order tensors present Shiah *et al* (2010b). Together with the first order derivatives, they are required in the evaluation of the stresses at the interior point of the body in BEM, using Somugliana's identity, and this implementation has been successfully achieved as well for 3D general anisotropy. The present paper provides further demonstration of this success. Two numerical examples are presented in which the solutions are compared with those obtained by FEM. The relative computational efficiency of the revised formulation is also examined, when compared with Lee's previous approach, Tan *et al* (2009) to obtain the 2^{nd} derivatives of the Green's function with a finite difference scheme. Before this, however, it is useful to first, provide a review of Somigliana's identity, the fundamental solution employed and the key steps for obtaining its derivatives. As has been explained in previous publications, because of their fully explicit, real variable forms, there are no special considerations required for the numerical evaluation of the fundamental solution and its derivatives employed here. The basic BEM numerical formulation is the same as that developed for 3D isotropic elasticity; hence details of this will not be presented here.

2 Somigliana's identity and fundamental solutions of 3D anisotropic elastic bodies

In BEM linear elastic stress analysis, the displacements and stresses at an interior point of the solid are obtained as a secondary process after the boundary integral equation (BIE), which relates the displacements, u_i, to the tractions, t_i, on the surface S of the domain, has been numerically solved for all their unknown values. For the displacements at an interior point, p, it involves evaluating the discretised form of Somigliana's identity which can be written as follows in the absence of body forces or thermal loads:

$$C_{ij}u_i(P) + \int_S u_i(Q)T_{ij}(P,Q)dS = \int_S t_i(Q)U_{ij}(P,Q)dS \tag{1}$$

where $U_{ij}(P,Q) \equiv \mathbf{U}$, and $T_{ij}(P,Q)$ represent the fundamental solutions of displacements and tractions, respectively, in the x_i-direction at the field point Q due to a unit load in the x_j-direction at P in a homogeneous infinite body. The corresponding stresses may be obtained using the generalized Hooke's law:

$$\sigma_{ij} = C_{ijmn}\left(u_{m,n} + u_{n,m}\right)/2 \tag{2}$$

in which the 1^{st}-order derivatives of displacements are obtained by differentiating

Eq. (1)

$$u_{i,k}(p) + \int_S u_i(Q) T_{ij,k}(p,Q) = \int_S t_i(Q) u_{ij,k}(p,Q) dS \tag{3}$$

The Green's function for displacements in 3D anisotropic bodies derived by Ting and Lee (1997) as implemented by Tan *et al.* (2009) can be expressed in simple closed-form as

$$\mathrm{U}(\mathbf{x}) = \frac{1}{4\pi r}\mathbf{H}[\mathbf{x}] = \frac{1}{|\mathbf{T}|}\sum_{\mathrm{n}=0}^{4} \mathrm{q_n}\hat{\mathbf{\Gamma}}^{(\mathrm{n})}, \tag{4}$$

where r is the radial distance between the load and field point, $\mathbf{H}[\mathbf{x}]$is the Barnett-Lothe tensor, and the expressions for$|\mathbf{T}|$, $\hat{\mathbf{\Gamma}}^{(\mathrm{n})}$ and $\mathrm{q_n}$ may be found in Ting and Lee (1997) and Tan *et al* (2009). As has been previously reported, the numerical evaluation of this Green's function is relatively straightforward. The numerical evaluation of T_{ij} is also required in solving the BIE and when evaluating Eq. (1). It may be carried out using the following well-known traction-stress and stress-strain relations, respectively:

$$T_{ij} = \sigma_{ik}^{(j)} N_k, \tag{5}$$

$$\sigma_{ik}^{(j)} = C_{ikmn}\left(U_{mj,n} + U_{nj,m}\right)/2 \tag{6}$$

In Eq. (5), $\sigma_{ik}^{(j)}$are the stresses at a field point due to a unit concentrated force applied in the x_j direction at the source point, and N_k are components of the outward normal of the surface at Q. From Eqs. (3) - (6) above, it is clear that the 1^{st} - and 2^{nd} -order derivatives of $\mathbf{U}$must be obtained. Upon revisiting this problem following the work in Shiah *et al* (2008), Lee (2009) suggested that the partial derivatives be obtained in a spherical coordinate system as an intermediate step and the chain rule then employed, instead of directly differentiating the fundamental solution in the Cartesian coordinate system, as follows,

$$U_{ij,l} = \frac{\partial U_{ij}}{\partial r}\frac{\partial r}{\partial x_l} + \frac{\partial U_{ij}}{\partial \theta}\frac{\partial \theta}{\partial x_l} + \frac{\partial U_{ij}}{\partial \varphi}\frac{\partial \varphi}{\partial x_l} \tag{7}$$

$$U_{ij,kl} = \frac{\partial U_{ij,k}}{\partial r}\frac{\partial r}{\partial x_l} + \frac{\partial U_{ij,k}}{\partial \theta}\frac{\partial \theta}{\partial x_l} + \frac{\partial U_{ij,k}}{\partial \varphi}\frac{\partial \varphi}{\partial x_l}. \tag{8}$$

The partial derivatives above can be expressed as follows:

$$\frac{\partial U_{ij}}{\partial r} = \frac{-U_{ij}}{r}, \quad \frac{\partial U_{ij}}{\partial \theta} = \frac{I'_{ij} - J'_{ij}}{4\pi^2 r}, \quad \frac{\partial U_{ij}}{\partial \varphi} = \frac{I''_{ij} - J''_{ij}}{4\pi^2 r} \tag{9}$$

$$\frac{\partial U_{ij,k}}{\partial r} = \frac{\partial^2 U_{ij}}{\partial r^2}\frac{\partial r}{\partial x_k} + \frac{\partial U_{ij}}{\partial r}\frac{\partial}{\partial r}\left(\frac{\partial r}{\partial x_k}\right) + \frac{\partial^2 U_{ij}}{\partial r \partial \theta}\frac{\partial \theta}{\partial x_k}$$
$$+ \frac{\partial U_{ij}}{\partial \theta}\frac{\partial}{\partial r}\left(\frac{\partial \theta}{\partial x_k}\right) + \frac{\partial^2 U_{ij}}{\partial r \partial \phi}\frac{\partial \phi}{\partial x_k} + \frac{\partial U_{ij}}{\partial \phi}\frac{\partial}{\partial r}\left(\frac{\partial \phi}{\partial x_k}\right),$$

$$\frac{\partial U_{ij,k}}{\partial \theta} = \frac{\partial^2 U_{ij}}{\partial r \partial \theta}\frac{\partial r}{\partial x_k} + \frac{\partial U_{ij}}{\partial r}\frac{\partial}{\partial \theta}\left(\frac{\partial r}{\partial x_k}\right) + \frac{\partial^2 U_{ij}}{\partial \theta^2}\frac{\partial \theta}{\partial x_k} + \frac{\partial U_{ij}}{\partial \theta}\frac{\partial}{\partial \theta}\left(\frac{\partial \theta}{\partial x_k}\right)$$
$$+ \frac{\partial^2 U_{ij}}{\partial \theta \partial \phi}\frac{\partial \phi}{\partial x_k} + \frac{\partial U_{ij}}{\partial \phi}\frac{\partial}{\partial \theta}\left(\frac{\partial \phi}{\partial x_k}\right),$$
$$\frac{\partial U_{ij,k}}{\partial \phi} = \frac{\partial^2 U_{ij}}{\partial r \partial \phi}\frac{\partial r}{\partial x_k} + \frac{\partial U_{ij}}{\partial r}\frac{\partial}{\partial \phi}\left(\frac{\partial r}{\partial x_k}\right) + \frac{\partial^2 U_{ij}}{\partial \theta \partial \phi}\frac{\partial \theta}{\partial x_k}$$
$$+ \frac{\partial U_{ij}}{\partial \theta}\frac{\partial}{\partial \phi}\left(\frac{\partial \theta}{\partial x_k}\right) + \frac{\partial^2 U_{ij}}{\partial \phi^2}\frac{\partial \phi}{\partial x_k} + \frac{\partial U_{ij}}{\partial \phi}\frac{\partial}{\partial \phi}\left(\frac{\partial \phi}{\partial x_k}\right); \tag{10}$$

$$\frac{\partial^2 U_{ij}}{\partial r^2} = \frac{U_{ij}}{r^2} - \frac{\partial U_{ij}}{\partial r}, \quad \frac{\partial^2 U_{ij}}{\partial r \partial \theta} = -\frac{1}{r^2}\frac{\partial U_{ij}}{\partial \theta}, \quad \frac{\partial^2 U_{ij}}{\partial r \partial \varphi} = -\frac{1}{r^2}\frac{\partial U_{ij}}{\partial \varphi},$$
$$\frac{\partial^2 U_{ij}}{\partial \theta^2} = \frac{1}{4\pi^2 r}\left(\frac{\partial I'_{ij}}{\partial \theta} - \frac{\partial J'_{ij}}{\partial \theta}\right), \quad \frac{\partial^2 U_{ij}}{\partial \phi^2} = \frac{1}{4\pi^2 r}\left(\frac{\partial I''_{ij}}{\partial \phi} - \frac{\partial J''_{ij}}{\partial \phi}\right),$$
$$\frac{\partial^2 U_{ij}}{\partial \theta \partial \phi} = \frac{1}{4\pi^2 r}\left(\frac{\partial I''_{ij}}{\partial \theta} - \frac{\partial J''_{ij}}{\partial \theta}\right) \tag{11}$$

It has been shown in Shiah *et al* (2010a) that the quantities, I'_{ij}, I''_{ij}, J'_{ij}, J''_{ij}, which appear in the equations above can be reduced to relatively direct, algebraic expressions in terms of the Stroh's eigenvalues. The explicit, algebraic expressions for the component terms of $U_{ij,l}$ and $U_{ij,kl}$ have also been derived by the present authors and presented in Shiah *et al* (2010b) very recently. No tensors higher than the second order are present in any of the terms in these expressions. They are also easy and relatively efficient to evaluate because of their simple algebraic forms, but are nevertheless still fairly elaborate.

3 Numerical examples

Three numerical examples are presented here to further demonstrate the successful implementation of Somigliana's identity in BEM for obtaining the displacements and stresses at an internal point in a 3D generally anisotropic elastic body using the explicit-form Green's function and its derivatives describe above. They have been implemented into an existing BEM code which had been originally written for isotropic elasticity based on the quadratic isoparametric formulation. The material

used in both examples is niobium (*Nb*) crystal that has the following stiffness elastic constants:

$$C_{11}^{*} = 246\text{GPa}; \quad C_{12}^{*} = 134\text{GPa}; \quad C_{44}^{*} = 28.7\text{GPa}, \tag{12}$$

where the asterisks denote properties defined in the directions of the principal axes of the material.

Figure 1 shows the first example considered. It is a hollow thick-walled sphere with radius ratio R_2/R_1=3.0 subjected to uniform radial tensile stress σ_o= 1 on the outer surface. The BEM mesh employed has a total of 64 quadratic elements and 156 nodes; the exterior surface was modelled with just 16 triangular elements and 34 nodes. It should be remarked that advantage could have been taken of the symmetry of the material properties of the cubic medium, and the loading conditions; only a fraction of the physical problem needs then to be modelled. However, the whole sphere was modelled here in the BEM analysis as the mesh is employed for other studies involving more general anisotropic properties.

The problem is no longer axisymmetric in the anisotropic case. For the present purpose, only the resultant displacements ($u_t = \sqrt{u_1^2 + u_2^2 + u_3^2}$) and the von Mises equivalent stresses σ_{eq} are presented here for a few sample internal points on the

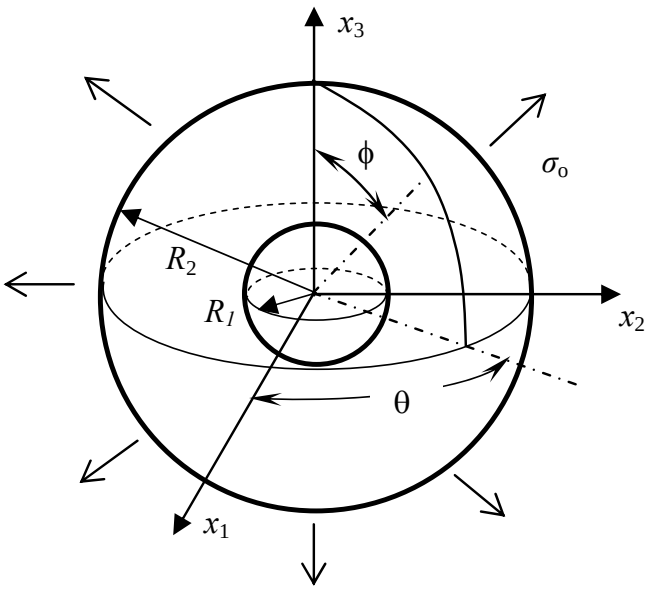

Figure 1: A thick-walled sphere subject to uniform radial stress at outer radius R_2.

equatorial plane, namely, at r/R_1=1.4 and 1.6. As a first check of the proper implementation of the formulation, the material is assumed to have isotropic elastic properties with Young's modulus E=1000 (units) and Poisson's ratio ν=0.3. This isotropic analysis was carried out by both the conventional isotropic formulation as wellas the present anisotropic algorithm using elastic stiffness constants corresponding to the isotropic properties. For comparison of the numerical results, the problem was also analyzed by the FEM using the commercial code ANSYS, where advantage was taken of the material symmetry. Only $1/8^{th}$ of the sphere was modelled in the FEM analysis, as shown in Fig. 2(b). This relatively refined mesh comprises of 433800 SOLID186 (quadratic) elements with 877982 nodes; it yielded exact solution to 4 decimal places in the isotropic case. Tables 1 and 2 show the normalized equivalent stress and resultant displacements, respectively, computed for the internal points. As can be seen, there is good agreement of the BEM and FEM results despite the relatively coarse BEM mesh used.

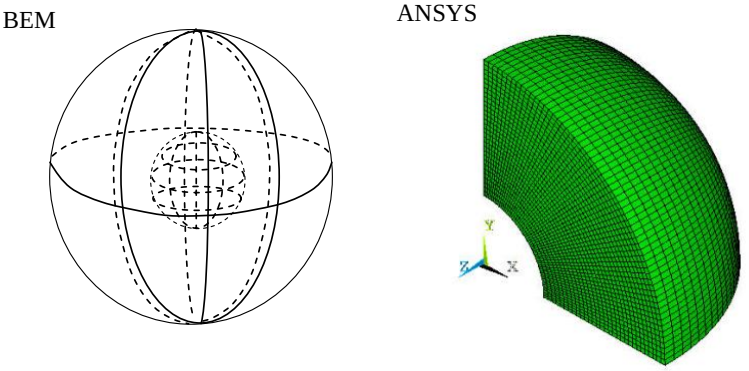

Figure 2: Mesh designs employed in the BEM and FEM analysis

The next example treated is a relatively short cantilever beam with length 12L and a square cross-section of side-lengths 2L, subjected to a uniform pressure σ_{22}= -P on its top surface. For the analysis, the material principal axes are deliberately rotated successively about the x_1-axis, x_2-axis, and x_3-axis counter-clockwise by 15^o, 30^o, and 45^o, respectively. This serves to demonstrate the capability of the algorithm to treat general anisotropy, as the rotations of the material principal axes yield the following fully populated stiffness matrix which has the characteristics of

Table 1: Normalized equivalent stress at the internal points

σ_{eq}/σ_0			ANSYS	BEM*	|%Diff.|	BEM**
Isotropic	r/R_1=1.4		0.5679	0.5748	1.23	0.5748
	r/R_1=1.6		0.3803	0.3904	2.66	0.3904
Anisotropic	r/R_1 =1.4	θ=0^o	0.6328	0.6423	1.51	N/A
		θ=15^o	0.6190	0.6277	1.41	
		θ=30^o	0.5801	0.5834	0.57	
		θ=45^o	0.5504	0.5494	0.18	
	r/R_1 =1.6	θ=0^o	0.4590	0.4756	3.61	
		θ=15^o	0.4377	0.4527	3.44	
		θ=30^o	0.3836	0.3905	1.80	
		θ=45^o	0.3505	0.3523	0.53	

*Anisotropic algorithm; **Isotropic algorithm

Table 2: Normalized resultant displacements at the internal points

Normalized displacement			ANSYS	BEM*	|%Diff.|	BEM**
(Isotropic) $u_t\ E/\sigma_0$	r/R_1=1.4		0.9251	0.9295	0.48	0.9295
	r/R_1=1.6		0.9277	0.9323	0.50	0.9323
(Anisotropic) $u_t C^*_{11}/\sigma_0$	r/R_1=1.4	θ=0^0	1.8458	1.8219	1.29	N/A
		θ=15^0	1.7725	1.7566	0.90	
		θ=30^0	1.6067	1.6035	0.20	
		θ=45^0	1.5108	1.5104	0.03	
	r/R_1=1.6	θ=0^0	1.7811	1.7545	1.49	
		θ=15^0	1.6926	1.6755	1.01	
		θ=30^0	1.4982	1.4968	0.09	
		θ=45^0	1.3903	1.3932	0.21	

*Anisotropic algorithm; **Isotropic algorithm

a generally anisotropic solid:

$$\mathbf{C} = \begin{pmatrix} 218.76 & 153.52 & 141.72 & -10.01 & 0.40 & 7.21 \\ 153.52 & 209.89 & 150.59 & -2.21 & 0.96 & -0.18 \\ 141.72 & 150.59 & 221.69 & 12.22 & -1.36 & -7.04 \\ -10.01 & -2.21 & 12.22 & 45.29 & -7.04 & 0.96 \\ 0.40 & 0.96 & -1.36 & -7.04 & 36.42 & -10.01 \\ 7.21 & -0.18 & -7.04 & 0.96 & -10.01 & 48.22 \end{pmatrix} \text{ GPa.} \tag{13}$$

The BEM and FEM meshes employed are shown in Figure 3. With the beam fixed completely at x_3=0, the normalized transverse displacements along the x_3-axis ob-

tained from both methods are shown in Figure 4. The results of σ_{33}/P and von Mises equivalent stress, σ_{eq}/P, for some internal points in the x_1= 0 plane at x_3=4L and 6L are listed in Table 3. It can be seen that the agreement between the results of the two different numerical methods is very good indeed.

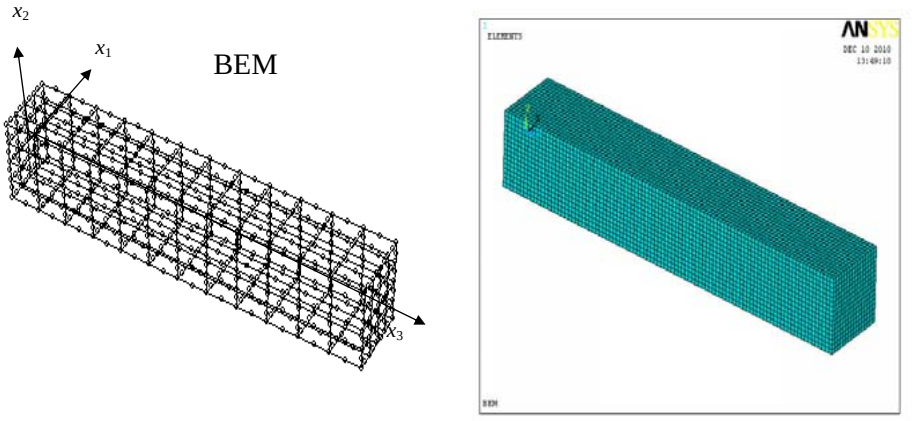

Figure 3: Numerical models for the anisotropic beam: BEM- 224 elements with 674 nodes; ANSYS- 24576 SOLID186 elements with 108545 nodes.

Table 3: Values of the normalized stress, σ_{33}/P, and normalized equivalent stress, σ_{eq}/P, at some points across the section at x_3=4L and 6L; x_1= 0.

			x_2= -L	x_2=-0.5L	x_2=0	x_2= 0.5L	x_2= +L
$\frac{\sigma_{33}}{P}$	x_3= 4L	FEM	-47.802	-24.089	-0.852E-04	24.088	47.802
		BEM	-47.554	-24.013	0.0104	24.033	47.548
		|%Diff.|	0.52	0.31	N/A	0.23	0.53
	x_3= 6L	FEM	-26.802	-13.588	-0.358E-06	13.588	26.802
		BEM	-26.614	-13.543	0.005	13.552	26.607
		|%Diff.|	0.70	0.33	N/A	0.26	0.73
$\frac{\sigma_{eq}}{P}$	x_3= 4L	FEM	47.802	25.253	10.431	25.739	48.311
		BEM	47.552	25.181	10.394	25.687	48.054
		|%Diff.|	0.52	0.28	0.36	0.20	0.53
	x_3= 6L	FEM	26.803	14.730	7.831	15.207	27.316
		BEM	26.614	14.687	7.804	15.173	27.124
		|%Diff.|	0.70	0.29	0.36	0.22	0.70

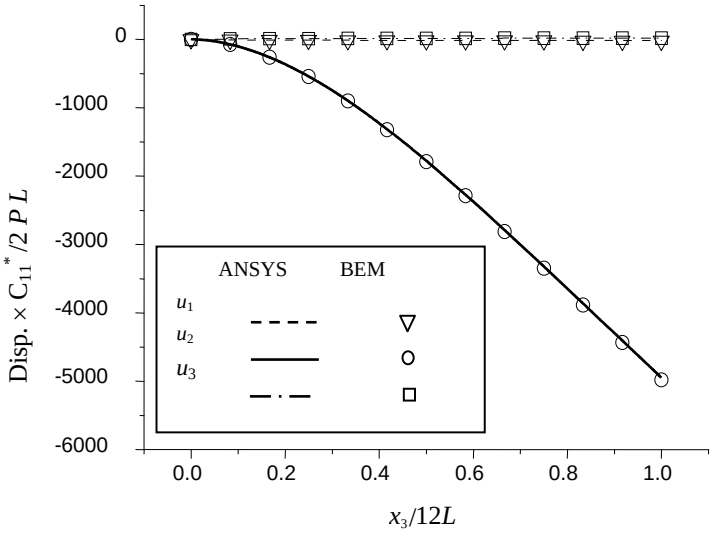

Figure 4: Variations of the normalized displacements along the x_3-axis of the anisotropic beam.

To check the relative computational efficiency of the present BEM approach *vis-a-vis* that of the previous algorithm given in terms of high order tensors Tan *et al* (2009), the CPU-time for the analysis of the cantilever beam problem using a i7-series desktop PC are compared. With the latter algorithm, the finite difference scheme is employed to calculate the second-order derivatives of the Green's function. The CPU-times recorded for the both approaches are normalized with respect to that for the computer run for the corresponding isotropic analysis. Figure 5 shows variations of the normalized CPU-times with the number of internal points for the analysis. It can be seen that the present approach is indeed significantly more efficient than that using the previous algorithm Tan *et al* (2009).

The third example considered here is as shown in Figure 6. It is a cylindrical bar with a spherical cavity fixed at one end and subjected to a uniform unit tensile load at the other end. The material properties used in the analysis are the same as those treated in the previous example, as given in Eq. 13. The case considered is for $a/R = 0.4$, $H/R = 2$. The determination of the boundary solutions for this stress concentration problem using BEM has been presented in Tan *et al* (2009). The resultant normalized displacements and the normalized equivalent stresses at a series of points around the circle at radius $r = 0.6R$ are obtained here. The mesh designs employed in BEM and FEM are shown in Fig. 7. Table 4 lists the results

obtained using the two techniques. It can be seen that they are, again, in very good agreement.

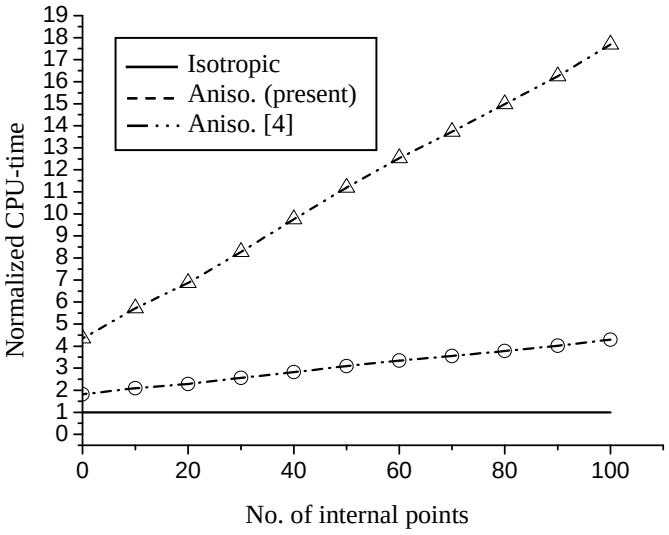

Figure 5: Normalized CPU-time varying with number of internal test points.

Table 4: Computed resultant displacement and normalized equivalent stress at interior points on a circle at $r/R = 0.6$ in the $x_3 = 0$ plane.

	$\delta = \sqrt{u_1^2 + u_2^2 + u_3^2}(*10^{-9})$			σ_{eq}/σ_o		
θ	FEM	BEM	|%Diff.|	FEM	BEM	|%Diff.|
0^o	0.1096	0.1070	2.37	1.2226	1.2140	0.71
45^o	0.1209	0.1183	2.14	1.2117	1.1994	1.01
90^o	0.1313	0.1286	2.05	1.2008	1.1903	0.87
135^o	0.1324	0.1295	2.18	1.2156	1.2049	0.88
180^o	0.1180	0.1152	2.31	1.2076	1.1971	0.87
225^o	0.1041	0.1013	2.72	1.2242	1.2146	0.78
270^o	0.1026	0.0996	2.89	1.232	1.2256	0.52
315^o	0.1050	0.1021	2.67	1.2398	1.2325	0.59

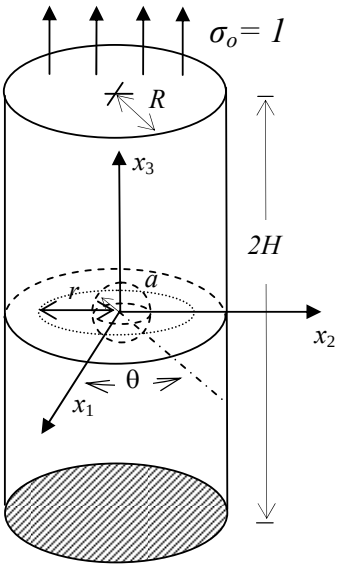

Figure 6: A cylinder with a spherical cavity under remote tension

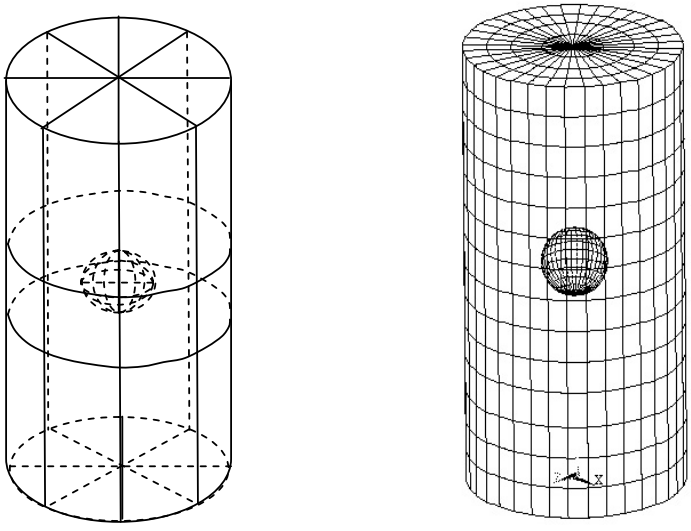

(a) (b)

Figure 7: Mesh designs: (a) 88 elements with 228 nodes for BEM; (b) 2940 SOLID186 elements with 6826 nodes for ANSYS FEM.

4 Conclusions

The first- and second-order derivatives of the Green's function by Ting and Lee (1997) for the displacements in a 3D generally anisotropic elastic solid have been derived using a revised approach suggested by Lee (2009).These fundamental solutions are required in the formulation of the BEM; the latter, in particular, are needed for obtaining the stresses at an interior point of the elastic body upon differentiating Somigliana's displacement identity. Three numerical examples have been presented in this paper to further demonstrate their successful implementation into a BEM code for internal point solutions. The numerical results for these BEM solutions obtained using the present formulations showed very good agreement indeed with those obtained using ANSYS-FEM analysis. A comparison of the CPU runtimes of the problems treated using the present algorithm and a previous approach has also been conducted. It clearly shows the superior efficiency of the present formulation outlined in this paper.

Acknowledgement: The authors gratefully acknowledge the financial support from the National Science and Engineering Research Council of Canada and the National Science Council of Taiwan (NSC 99-2221-E-035-027-MY3).

References

Benedetti, I.; Milazzo, A.; Aliabadi, M.H. (2009): A fast dual boundary element method for 3D anisotropic crack problems. *Int. J. Numer. Methods Engng.*, 1356-1378.

Buroni, F.C.; Saez, A. (2010): Three-dimensional Green's function and its derivative for materials with general anisotropic magneto-electro-elastic coupling. *Proc. Royal Soc. A*, 466, 515-537.

Lee,V.G. (2009): Derivatives of the three-dimensional Green's functions for anisotropic materials. *Int. J. Solids Struct.*, 46, 3471-3479.

Lifshitz, I.M.; Rosenzweig, **L.N.** (1947): Construction of the Green tensor for the fundamental equation of elasticity theory in the case of unbounded elastically anisotropic medium, *Zh. Eksp. Teor. Fiz.*, 17, 783-791.

Shiah, Y.C.; Tan, C.L.; Sun, W.X.; Chen, Y.H. (2010a): On the displacement derivatives of the three-dimensional Green's function for generally anisotropic bodies. *Advances in Boundary Element Techniques XI*, *Proc. BeTeq 2010 Conf.*, *Berlin*, Ch. Zhang, M.H. Aliabadi & M. Schanz (eds.), E.C. Ltd. (U.K.), pp. 426-432.

Shiah, Y.C.; Tan, C.L.; Lee, R.F. (2010b): Interior point solutions for displacementsand stresses in 3D anisotropic elastic solids using the boundary element method.

CMES: Computer Modeling in Engineering and Sciences, 69, 167-197.

Shiah, Y.C.; Tan, C.L.; Lee, V.G. (2008): Evaluation of explicit-form fundamental solutions for displacements and stresses in 3D anisotropic elastic solids. *CMES: Computer Modeling in Engineering & Sciences*, 34, 205-226.

Tan, C.L.; Shiah, Y.C.; Lin, C.W. (2009): Stress analysis of 3D generally anisotropic elastic solids using the boundary element method. *CMES: Computer Modeling in Engineering & Sciences*, 41, 195-214.

Ting, T.C.T.; Lee,V.G. (1997):The three-dimensional elastostic Green's function for general anisotropic linear elastic solid. *Q. J. Mech. Appl. Math.*, 50, 407-426.

Wilson, R.B.; Cruse, T.A. (1978): Efficient implementation of anisotropic three dimensional boundary integral equation stress analysis. *Int. J. Numer. Methods Engng.*, 12, 1383-1397.